PLOS BIOLOGY

SHORT REPORTS

Ancestral SARS-CoV-2, but not Omicron, replicates less efficiently in primary pediatric nasal epithelial cells

Yanshan Zhu[1], Keng Yih Chew[1], Melanie Wu[1], Anjana C. Karawita[1], Georgina McCallum[1], Lauren E. Steele[1], Ayaho Yamamoto[2], Larisa I. Labzin[3], Tejasri Yarlagadda[4], Alexander A. Khromykh[1,5], Xiaohui Wang[3], Julian D. J. Sng[1], Claudia J. Stocks[3], Yao Xia[6,7], Tobias R. Kollmann[8], David Martino[8], Merja Joensuu[9,10], Frédéric A. Meunier[9,11], Giuseppe Balistreri[11,12], Helle Bielefeldt-Ohmann[1,5], Asha C. Bowen[8,13,14,15], Anthony Kicic[8,16,17], Peter D. Sly[2,5], Kirsten M. Spann[4], Kirsty R. Short[1,5]*

1 School of Chemistry and Molecular Biosciences, The University of Queensland, Brisbane, Queensland, Australia, **2** Child Health Research Centre, The University of Queensland, South Brisbane, Queensland, Australia, **3** Institute for Molecular Bioscience, The University of Queensland, Brisbane, Queensland, Australia, **4** Centre for Immunology and Infection Control, Faculty of Health, School of Biomedical Sciences, Queensland University of Technology, Brisbane, Queensland, Australia, **5** Australian Infectious Diseases Research Centre, Global Virus Network Centre of Excellence, Brisbane, Queensland, Australia, **6** School of Science, Edith Cowan University, Joondalup, Western Australia, Australia, **7** School of Biomedical Sciences, The University of Western Australia, Perth, Western Australia, Australia, **8** Wal-yan Respiratory Research Centre, Telethon Kids Institute, The University of Western Australia, Perth, Western Australia, Australia, **9** Clem Jones Centre for Ageing Dementia Research, Queensland Brain Institute, The University of Queensland, Brisbane, Queensland, Australia, **10** Australian Institute for Bioengineering and Nanotechnology, The University of Queensland, Brisbane, Queensland, Australia, **11** School of Biomedical Sciences, The University of Queensland, Brisbane, Queensland, Australia, **12** Department of Virology, Faculty of Medicine, University of Helsinki, Helsinki, Finland, **13** Department of Infectious Diseases, Perth Children's Hospital, Nedlands, Perth, Western Australia, Australia, **14** Wesfarmers Centre for Vaccines and Infectious Diseases, Telethon Kids Institute, The University of Western Australia, Perth, Western Australia, Australia, **15** Menzies School of Health Research, Charles Darwin University, Darwin, Northern Territory, Australia, **16** Occupation and Environment, School of Public Health, Curtin University, Perth, Western Australia, Australia, **17** Centre for Cell Therapy and Regenerative Medicine, School of Medicine and Pharmacology, The University of Western Australia, Perth, Western Australia, Australia

* k.short@uq.edu.au

Citation: Zhu Y, Chew KY, Wu M, Karawita AC, McCallum G, Steele LE, et al. (2022) Ancestral SARS-CoV-2, but not Omicron, replicates less efficiently in primary pediatric nasal epithelial cells. PLoS Biol 20(8): e3001728. https://doi.org/10.1371/journal.pbio.3001728

Academic Editor: Bill Sugden, University of Wisconsin-Madison, UNITED STATES

Received: May 26, 2022

Accepted: June 24, 2022

Published: August 1, 2022

Data Availability Statement: All relevant data are within the paper and its Supporting information file. RNA-seq data is deposited at European Nucleotide Archive under the project– PRJEB43102. The scripts used for RNA-seq data analysis including differential gene expression and gene set enrichment analysis can be found in https://github.com/akaraw/Yanshan_Zhu_et_al.

Funding: This work is supported by the Australia Research Council (Discovery Early Career Researcher Award DE190100565 to M.J.), The

Abstract

Children typically experience more mild symptoms of Coronavirus Disease 2019 (COVID-19) when compared to adults. There is a strong body of evidence that children are also less susceptible to Severe Acute Respiratory Syndrome Coronavirus 2 (SARS-CoV-2) infection with the ancestral viral isolate. However, the emergence of SARS-CoV-2 variants of concern (VOCs) has been associated with an increased number of pediatric infections. Whether this is the result of widespread adult vaccination or fundamental changes in the biology of SARS-CoV-2 remain to be determined. Here, we use primary nasal epithelial cells (NECs) from children and adults, differentiated at an air–liquid interface to show that the ancestral SARS-CoV-2 replicates to significantly lower titers in the NECs of children compared to those of adults. This was associated with a heightened antiviral response to SARS-CoV-2 in the NECs of children. Importantly, the Delta variant also replicated to

National Health and Medical Research Council (Project grant APP2010917 to F.A.M. and G.B.; Senior research Fellowship APP1155794 to F.A.M; APP1124612 to LL; 2010757 to KYC and LL; NHMRC investigator grant 2007919 to K.R.S.) the Australian Infectious Diseases Research Centre (COVID-19 seed grant to A.A.K) and Academy of Finland and COVID19 research donations (Grant 318434 to G.B.). This program has in part been funded by the Western Australian Future Health Research & Innovation Fund. The funders had no role in study design, data collection and analysis, decision to publish, or preparation of the manuscript.

Competing interests: I have read the journal's policy and the authors of this manuscript have the following competing interests: KRS is a consultant for Sanofi, Roche and NovoNordisk. The opinions and data presented in this manuscript are of the authors and are independent of these relationships.

Abbreviations: ACE2, angiotensin-converting enzyme 2; ALI, air liquid interface; ARDS, acute respiratory distress syndrome; COVID-19, Coronavirus Disease 2019; DEG, differentially expressed gene; DGE, differential gene expression; ECL, enhanced chemiluminescence; GAPDH, glyceraldehyde 3-phosphate dehydrogenase; GO, gene ontology; h.p.i, hours post-infection; HE, hematoxylin–eosin; HPRT, hypoxanthine-guanine phosphoribosyltransferase; HRP, horseradish peroxidase; NEC, nasal epithelial cell; NP, nucleoprotein; ORF, open reading frame; PAS, periodic acid–Schiff; qRT-PCR, quantitative reverse transcription PCR; ROI, region of interest; SARS-CoV-2, Severe Acute Respiratory Syndrome Coronavirus 2; TMPRSS2, transmembrane serine protease 2; VOC, variant of concern; ZO-1, zonal occludens-1.

significantly lower titers in the NECs of children. This trend was markedly less pronounced in the case of Omicron. It is also striking to note that, at least in terms of viral RNA, Omicron replicated better in pediatric NECs compared to both Delta and the ancestral virus. Taken together, these data show that the nasal epithelium of children supports lower infection and replication of ancestral SARS-CoV-2, although this may be changing as the virus evolves.

Introduction

Severe Acute Respiratory Syndrome Coronavirus 2 (SARS-CoV-2), the causative agent of Coronavirus Disease 2019 (COVID-19), causes a broad range of clinical symptoms, ranging from asymptomatic infection to potentially fatal acute respiratory distress syndrome (ARDS). Children typically experience mild symptoms of COVID-19 when compared to adults [1]. There is also a significant body of evidence with the ancestral viral strain that children are less susceptible to SARS-CoV-2 infection and less likely to transmit the virus [2]. These findings have been echoed in multiple single site studies where, both within and outside of households, the infection rate of the ancestral SARS-CoV-2 among children <10 years old is significantly lower than that of adults [3,4]. Reduced SARS-CoV-2 infection and transmission is also observed in juvenile ferrets compared to their older counterparts [5].

The reasons for less frequent SARS-CoV-2 infection and symptoms in children infected with the ancestral virus strain remain unclear and may be influenced by a multitude of factors. There is evidence to suggest that nasal epithelial cells (NECs), the first site of infection, are fundamentally different in children compared to adults. Gene expression studies using the nasal epithelium of healthy individuals suggest that the transcript for the SARS-CoV-2 receptor, angiotensin-converting enzyme 2 (*ACE2*), is expressed at lower levels in children than in adults [6]. However, this has yet to be validated on a protein level. Moreover, this does not appear to be the case in all patient cohorts [7,8]. Following binding of the SARS-CoV-2 spike protein to ACE2, the host surface transmembrane serine protease 2 (TMPRSS2) is also involved in viral entry into the cell [9]. NECs from children express less *TMPRSS2* mRNA than those from adults, which may contribute to less frequent pediatric infections with SARS-CoV-2 [10]. However, this has also yet to be confirmed at protein level. In addition to differential receptor expression, pediatric and adult NECs may also mount fundamentally different innate immune response to SARS-CoV-2. Recent RNA sequencing of the whole epithelium from pediatric and adult proximal airways suggests that there is a higher expression of genes associated with inflammation and the antiviral response in children compared to adults [11,12]. While increased inflammation and interferon production have previously been associated with elevated COVID-19 severity [13], it is important to note that such studies refer to the inflammatory response in the lower respiratory tract, where any immunopathology may lead to respiratory distress [14]. In contrast, inflammation in the upper respiratory tract plays an important role in controlling early viral replication. Specifically, elevated levels of type I IFN effectively inhibit the replication of SARS-CoV-2 across multiple studies [15–17]. Consistent with these data, nasopharyngeal swabs from SARS-CoV-2-infected children display elevated levels of interferons and inflammatory markers compared to those of SARS-CoV-2-infected adults [7].

During the course of the SARS-CoV-2 pandemic, the ancestral virus has undergone significant mutations resulting in the emergence of variants of concern (VOCs) such as Delta and

Omicron. These VOCs have multiple mutations in the spike protein, the N protein, and various open reading frames (ORFs) of the virus, which has resulted in their increased transmissibility and potentially differing clinical outcome [18]. The growing dominance of VOCs has raised speculation that the epidemiology of SARS-CoV-2 infection has fundamentally changed, specifically in terms of the role that children play in spreading the virus. For example, epidemiological household transmission studies have found little evidence of differential susceptibility to Delta in children compared to adults [19,20]. In addition, data from South Africa [21] and the United States [22] found a rapid increase in pediatric COVID-19-related hospital admission associated with the Omicron wave. These data may suggest that VOCs have evolved such that they are now able to evade any protection that the innate immune response has previously afforded children in terms of infection with the ancestral virus [7,12,18,23]. However, the extrapolation of epidemiology studies to fundamental immunology are complicated by the fact that the Delta and Omicron waves emerged at a time when a large percentage of the adult population were eligible for vaccination while vaccination of children <12 years old often lagged behind. Therefore, the role of pediatric innate immunity during VOC infection remains undefined.

Here, we use primary NECs, differentiated at an air–liquid interface, to investigate differential infection kinetics and antiviral responses to SARS-CoV-2 (ancestral and VOCs) infection in children and adults.

Results

Pediatric nasal epithelial cells are phenotypically different to adult nasal epithelial cells

To investigate the role of NECs in SARS-CoV-2 infection, adult and pediatric NECs were differentiated at an air–liquid interface. The phenotype of these cells at baseline (i.e., prior to infection) was then assessed. Adult NECs grew as a pseudostratified columnar epithelium with scattered goblet cells and ciliated epithelial cells (Fig 1A). Pediatric NECs also grew as a pseudostratified columnar epithelium with ciliated epithelial cells and goblet cells (Fig 1A). However, scattered cells with pyknotic nucleus and condensed cytoplasm were also observed, leaving pseudocysts in the epithelium (S1 Fig). This is potentially indicative of higher cell turnover and metabolic rate in the pediatric epithelial cells [24,25]. Immunofluorescence images of zonal occludens-1 (ZO-1)-stained NECs showed that tight junction proteins were built up closely toward the apical region of both adult and pediatric cells (Fig 1B). Periodic acid–Schiff (PAS) staining indicated the presence of mucus-producing cells (Fig 1A) in both pediatric and adult NECs. Consistent with these data, MUC5AC staining was detected exclusively on the apical layer, thus demonstrating mucus secretion by differentiated NECs (Fig 1B). Previous mRNA expression studies suggest that pediatric NECs express lower levels of *ACE2* and *TMPRSS2* compared to their adult counterparts [6,10]. However, these findings are inconsistent between patient cohorts and have not been investigated at a protein level [8]. Immunofluorescence staining suggested that pediatric NECs had a trend toward lower surface levels of ACE2 compared to their adult counterparts (Fig 1B and 1C). Accordingly, we sought to confirm these data using western blot on the NECs from a larger **number** of donors ($n = 5$) (Figs 1D, 1E and S3). While the same trend was observed by **western** blot (increased levels of ACE2 in adult NECs), this failed to reach statistical significance (Figs 1D, 1E and S3). There was no observable trend in TMPRSS2 levels between adult and pediatric NECs (Figs 1D, 1E and S3).

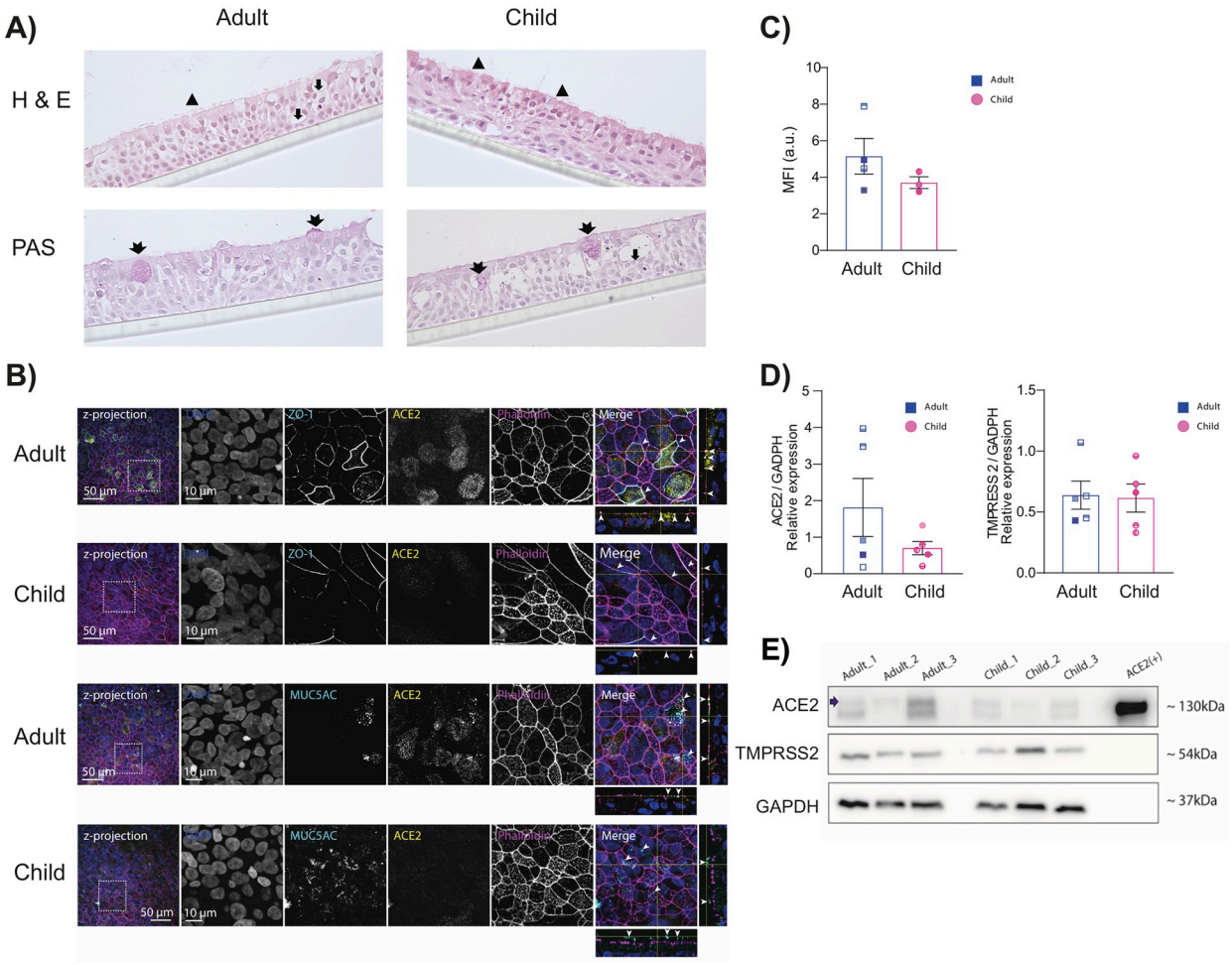

Fig 1. Pediatric nasal epithelial cells are phenotypically different to adult nasal epithelial cells. (**A**) Representative HE- and PAS-stained sections of pediatric and adult NECs culture differentiated at an air–liquid interface (representative of 2 adults (1 female, 1 male) and 3 pediatric (1 female, 2 males) donors). Arrowheads indicate ciliated cells, arrows indicate goblet cells, and double-tailed arrows indicate mucus-producing cells as determined by PAS staining. Images taken at 400× magnification. Each scale bar is equivalent of 150 μm. (**B**) Representative z-projections (150 optical sections) of pediatric and adult NECs cultures differentiated at an air–liquid interface and immunolabeled against endogenous ZO-1 and ACE2 (cyan and yellow, respectively, top panels) and MUC5AC and ACE2 (cyan and yellow, respectively, bottom panels). Cells were also stained with DAPI (blue) and phalloidin (magenta) to indicate the nucleus and actin filaments, respectively. The area in the dotted box in the images on left are shown magnified in the respective rows (10-μm bar applies to all images in the row). The merged image on right shows the orthogonal view of the z-stacks. The arrowheads indicate the ZO-1-stained profiles (top panels) and mucus secretion (MUC5AC) in the lower panels. (**C**) Quantification of ACE2 immunofluorescence as described in the Materials and methods. Mean ± SEM is shown. Each data point represents the average of 5 separate images taken from 1 donor (adult ($N = 4$, 2 females, 2 male) and pediatric ($N = 3$, 2 females, 1 male)). (**D**) Relative ACE2 and TMPRSS2 protein levels compared to GAPDH in adult (3 females, 2 males) and pediatric (3 females, 2 males) NECs. Each data point represents a different donor. Mean ± SEM is shown. (E) Representative western blot of NECs from 3 adult and 3 pediatric donors blotted for ACE2, TMPRSS2, and GAPDH. ACE2 is indicated with an arrow. Each donor is indicated by unique symbol that is used consistently throughout all figures. Data are contained in S1 Data, and raw western blot images are available in S1 Raw images. ACE2, angiotensin-converting enzyme 2; GAPDH, glyceraldehyde 3-phosphate dehydrogenase; HE, hematoxylin–eosin; NEC, nasal epithelial cell; PAS, periodic acid–Schiff; TMPRSS2, transmembrane serine protease 2; ZO-1, zonal occludens-1.

https://doi.org/10.1371/journal.pbio.3001728.g001

Pediatric nasal epithelial cells are less permissive to SARS-CoV-2 replication

We next sought to determine if pediatric NECs were less susceptible than adult NECs to SARS-COV-2 replication with the ancestral virus (QLD/02). Strikingly, significantly reduced SARS-CoV-2 replication was observed in pediatric NECs at 24 and 48 hours post-infection (h. p.i) (Fig 2A). Reduced SARS-CoV-2 N protein level was also observed in pediatric NECs at 24

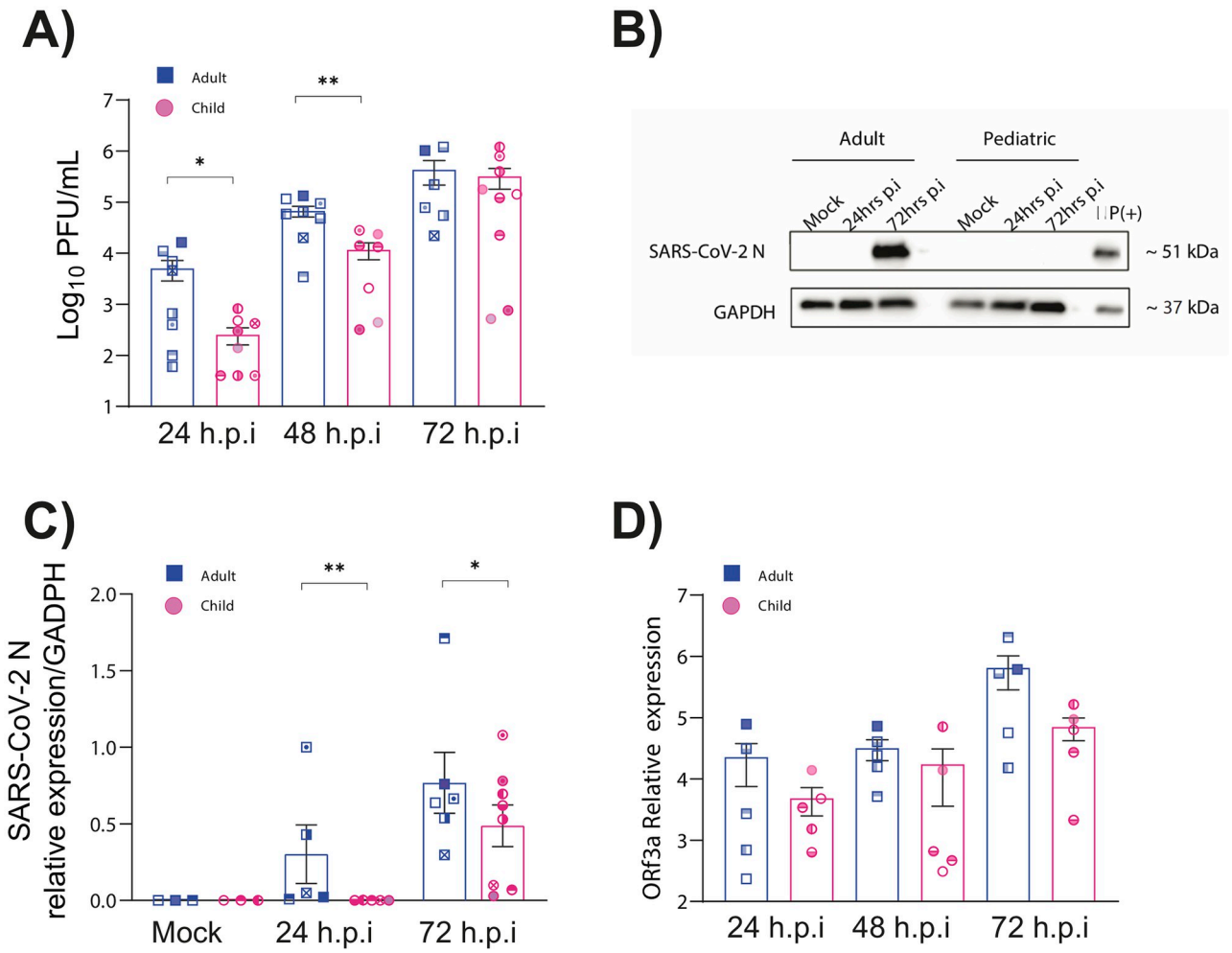

Fig 2. Lower replication of SARS-CoV-2 in pediatric nasal epithelial cells. (**A**) PFUs of SARS-CoV-2 (QLD02) from the apical surface of NECs ($N = 8$ adults: 5 females, 3 males and $N = 10$ children: 5 females, 5 males) obtained at 24, 48, and 72 h.p.i. Cells were infected with 1.25×10^5 PFU. (**B**) Representative western blot of adult and pediatric donor blotted for SARS-CoV-2 NP at various time points post-infection. All the western blot results for SARS-CoV-2 NP are shown as S2 Fig. (**C**) Relative SARS-CoV-2 NP levels compared to GAPDH in pediatric and adult NECs. * NP levels of 1 pediatric donor at 24 h.p.i are missing. (**D**) Expression of ORF3a RNA (log10) in infected cells at various time points relative to HPRT expression. Each donor is indicated by unique symbol that is used consistently throughout all figures. Mean ± SEM is shown. $p < 0.05^*$, $p < 0.01^{**}$. Statistical analysis performed as described in the Materials and methods. Data are contained in S1 Data, and raw western blot images are available in S1 Raw images. GAPDH, glyceraldehyde 3-phosphate dehydrogenase; HPRT, hypoxanthine-guanine phosphoribosyltransferase; h.p.i, hours post-infection; NEC, nasal epithelial cell; NP, nucleoprotein; PFU, plaque-forming unit; SARS-CoV-2, Severe Acute Respiratory Syndrome Coronavirus 2.

https://doi.org/10.1371/journal.pbio.3001728.g002

h.p.i and 72 h.p.i (Figs 2B, 2C and S2). RNA levels showed a similar pattern although no statistical significance was recorded (Fig 2D). After infection, there was also no significant difference in ACE2 levels between adult and pediatric donors (S3 Fig).

Pediatric nasal epithelial cells mount a strong antiviral response to SARS-CoV-2

To gain a further insight into the observed decrease of SARS-CoV-2 replication in pediatric NECs, RNA-seq was performed on infected adult and pediatric cells 72 h.p.i with the ancestral SARS-CoV-2 virus. PCA analysis showed that infected cells formed distinct clusters depending on whether they were derived from pediatric or adult donors (Fig 3A). Numerous differentially expressed genes were recorded in infected cells (Fig 3B). In infected pediatric NECs, gene

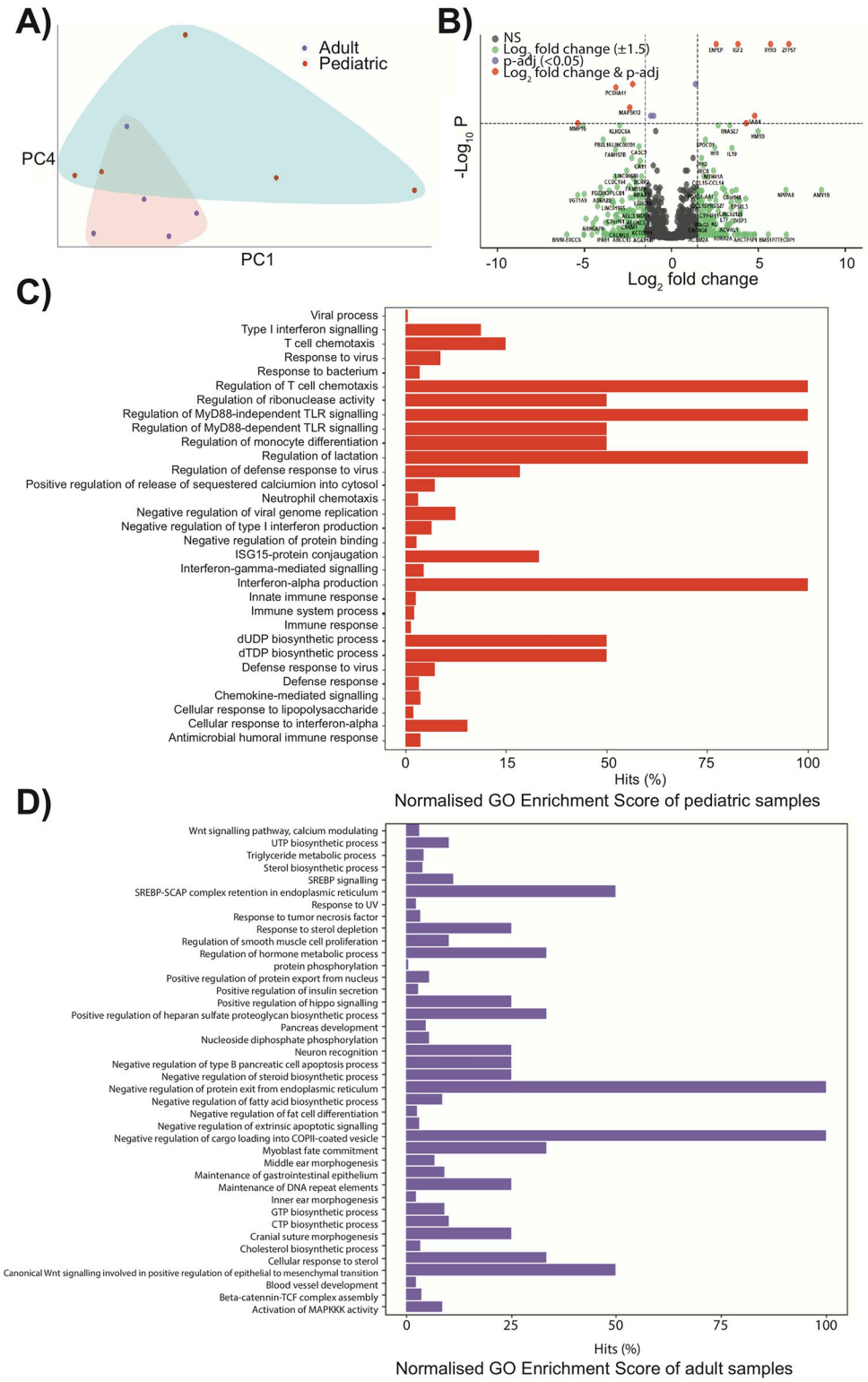

Fig 3. Pediatric epithelial cells have a different transcriptional response to SARS-CoV-2. (**A**) Principal component analysis for the global transcriptional response of naive pediatric and adult NECs. Data points represent individual donors ($N = 5$ adults: 4 females, 1 male and $N = 5$ pediatric donors: 2 females, 3 males). (**B**) Volcano plot illustrating DEGs of infected pediatric NECs compared to adult cells. DEGs statistically different between the 2 patient groups with a fold change of >1.5 are indicated in orange. DEGs statistically different between 2 groups with a fold change of

<1.5 are shown in purple. DEGs not statistically different between 2 groups with a fold change of >1.5 are shown in green. NS = not significant. (**C**) GO analysis of DEGs in infected pediatric NECs was displayed by the bar chart. The bars of significantly GO-enriched (overrepresented p value < 0.05) results were marked in red, x-axis reflects the gene count hits as a percentage over genes in each GO category; y-axis reflects different GO terms. (**D**) GO analysis of DEGs in adult NECs was displayed by the bar chart. The bars of significantly enriched GO (overrepresented p value < 0.05) enrichment results were marked in purple and represent the gene count hits (as a percentage over number of genes in a given category); y-axis reflects different GO terms. Data are contained in S1 Data. DEG, differentially expressed gene; GO, gene ontology; NEC, nasal epithelial cell; SARS-CoV-2, Severe Acute Respiratory Syndrome Coronavirus 2.

https://doi.org/10.1371/journal.pbio.3001728.g003

ontology (GO) enrichment analysis (Fig 3C) demonstrated a strong interferon response, with GO terms such as "viral process," "type I interferon signaling," "response to virus," "regulation of defense response to virus," "negative regulation of viral genome replication," "defense response to virus," and "cellular response to interferon alpha." None of these GO terms were identified among the top differentially expressed GO terms in adult cells infected with SARS-CoV-2 (Fig 3D). In contrast, GO terms such as "cellular response to sterol," "Wnt signalling pathway," and "response to tumor necrosis factor" were recorded. To confirm that these data were not restricted to a DESeq2 analysis, gene expression data were also analyzed using limma (S1 and S2 Tables). Once again, in infected pediatric NECs GO terms such as "response to virus," "cellular response to cytokine stimulus," and "defense response to virus" were recorded. In contrast, infected adult NECs were associated with GO terms such as "detection of stimulus involved in sensory perception" and "sensory perception." To further validate these data, we assessed gene expression by qPCR of 3 genes associated with inflammatory/antiviral response —interferon-induced protein with tetratricopeptide repeats 1 (*IFIT1*), C-X-C motif chemokine ligand 10 (*CXCL10*), and interferon-stimulated gene 15 (*ISG15*). Infected pediatric NECs had significantly higher levels of *IFIT1* compared to infected adult NECs (Fig 4A). Infected pediatric NECs also had a trend of increased IFN-alpha, IFN-beta, and CXCL10 protein levels following SARS-CoV-2 infection, although donor-to-donor variability precluded significance (Fig 4B–4D).

We next sought to investigate if we observed similar phenotype in pediatric epithelial cells infected with selected VOCs (Delta and Omicron). At 24 h.p.i, there were significantly high titers of infectious virus and viral RNA in adult epithelial cells infected with the ancestral virus (QLD02) and Delta compared to the epithelial cells of children (Fig 4E). Interestingly, while a similar (albeit not significant) trend was observed in Omicron infectious virus titers, there was no difference in Omicron RNA levels in pediatric versus adult NECs (Fig 4F).

Discussion

Large clinical data sets and systematic reviews suggest that children are less often infected with the ancestral SARS-CoV-2 and have less severe symptoms than adults [26–28]. However, the mechanisms driving these observations have been unclear. Here, we have provided the first experimental evidence that the pediatric nasal epithelium may play an important role in reducing the susceptibility of children to ancestral SARS-CoV-2.

Previous studies have suggested that the reduced susceptibility of children to SARS-CoV-2 infection is due to reduced mRNA expression of SARS-CoV-2 receptors ACE2 and TMPRSS2. Specifically, it has been proposed that the lower level of ACE2 and TMPRSS2 in pediatric upper airways epithelial cells limits disease severity and viral infectivity in children [6,29], although this has remained somewhat controversial [7,8]. In the present study, while there was a trend toward decreased ACE2 protein levels in pediatric NECs, there was significant donor-to-donor variability that precluded statistical significance. We interpret these data as

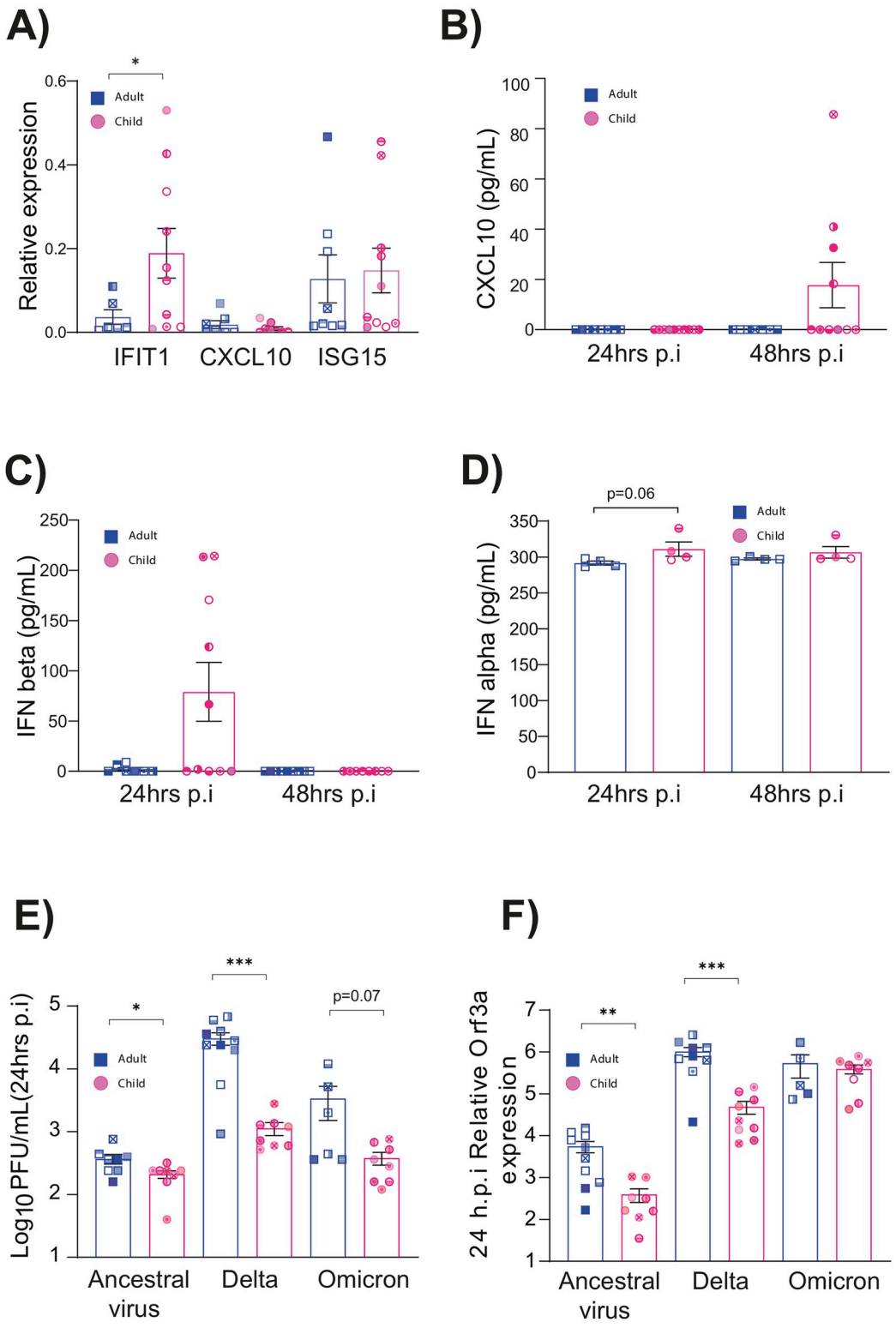

Fig 4. Pediatric epithelial cells have a stronger type I IFN response to viral infection. (**A**) Expression of interferon associated genes in ancestral SARS-CoV-2 (QLD02)-infected epithelial cells relative to uninfected controls (48 h.p.i). Each data point represents a different donor ($N = 8$ adults: 5 females, 3 males and $N = 10$ pediatric: 5 females, 5 males). Gene expression (fold change) was calculated using the ΔΔCt method relative to GAPDH expression. (**B–D**) Levels of IFN-alpha, IFN-beta, and CXCL10 in epithelial cell supernatant at 24 and 48 h.p.i with ancestral SARS-CoV-2 (QLD02). Mean ± SEM

is shown. $p < 0.05^{*}$, statistical analysis performed as described in the Materials and methods. Each donor is indicated by unique symbol that is used consistently throughout all figures. Number of donors shown in 4B and 4C ($N = 8$ adults: 5 females, 3 males and $N = 10$ children: 5 females, 5 males) and 4D ($N = 5$ adults: 4 females, 1 male and $N = 5$ children: 2 females, 3 males) were different. (**E**) Lower replication of SARS-CoV-2 Delta in pediatric nasal epithelial cells. PFUs of SARS-CoV-2 from the apical surface of nasal epithelial cells NECs obtained at 24 h.p.i. Cells were infected with 1.7×104 PFU of each of the respective viral variants. (**F**) Expression of ORF3a RNA in infected cells at relative to GAPDH expression. Each donor is indicated by unique symbol that is used consistently throughout all figures ($N = 10$ adults: 5 females, 5 males and $N = 10$ children: 5 females, 5 males). Mean ± SEM is shown. $p < 0.05^{*}$, $p < 0.01^{**}$. Statistical analysis performed as described in the Materials and methods. Data are contained in S1 Data. GAPDH, glyceraldehyde 3-phosphate dehydrogenase; h.p.i, hours post-infection; PFU, plaque-forming unit; SARS-CoV-2, Severe Acute Respiratory Syndrome Coronavirus 2.

https://doi.org/10.1371/journal.pbio.3001728.g004

suggesting that ACE2 levels may contribute to, but are not the sole factor, in the increased resistance of children to SARS-CoV-2.

Despite donor-to-donor differences in ACE2 expression, we consistently observed a significant reduction in ancestral SARS-CoV-2 (QLD02) replication in pediatric NECs compared to NECs of adults. Given that the nasal epithelium is the first site of SARS-CoV-2 infection, these data are consistent with the reduced number of SARS-CoV-2-infected children recorded in household and school transmission studies [30,31]. However, we recognize it is challenging to compare data from controlled experimental studies to data obtained from patient sampling, where it is difficult to control for time of sampling relative to the onset of infection. Rather, decreased viral replication in pediatric epithelial cells is consistent with experimental studies in ferrets where aged ferrets showed higher viral load and longer nasal virus shedding [5].

Consistent with reduced ancestral SARS-CoV-2 replication in the nasal epithelium of children, pediatric epithelial cells had a more pronounced pro-inflammatory response (compared to adult cells) following an ancestral SARS-CoV-2 infection. In particular, a pronounced interferon response and the expression of interferon stimulated genes (*ISGs*) were higher in infected pediatric, compared to adult, NECs. Increased *ISG* expression and the subsequent antiviral response may contribute to the reduced viral replication observed in pediatric cells. Importantly, unlike the lower respiratory tract, any resultant cell death or immunopathology in the upper respiratory tract is unlikely to lead to respiratory distress and therefore remains beneficial to the host [13]. These findings are consistent with those of Maughan and colleagues, who analyzed transcriptional profile of airway (tracheobronchial) epithelium and observed up-regulated type I and II *IFNs* associated genes in children [11]. Similarly, in the nasal fluid of children and adults presenting to the emergency department with SARS-CoV-2, there were significantly higher levels of *IFN-α2* in the fluid derived from children. Increased interferon signaling was also recorded in the nasopharyngeal transcriptome of children compared to that of adults during early SARS-CoV-2 infection [7].

The question remains as to why pediatric epithelial cells mount a stronger inflammatory and antiviral response to ancestral SARS-CoV-2 compared to adult cells. This may represent an adaptation to the increased antigenic challenge observed in childhood. Alternatively, it is possible that increased antigenic exposure in childhood "trains" nasal epithelium in children to mount a stronger pro-inflammatory response to any antigenic challenge. It is also possible that metabolic differences between pediatric and NECs (as potentially suggested by the different morphologies of the cells) could alter gene expression.

It is striking to note that the VOC Delta also replicated significantly better in the NECs of adults compared to those of children. These data suggest that any increase in pediatric infections during the Delta wave are unlikely to be due to the fact that the virus has substantially evaded the innate immune response of pediatric NECs and are instead more likely attributable to other factors (e.g., age-dependent differences in prior infection and/or vaccination).

Interestingly, the Delta variant replicated to higher titers in the NECs of both adults and children when compared to the ancestral virus. This is consistent with previous studies [32] and may be associated with the increased transmissibility of Delta compared to the ancestral virus. Interestingly, at least in adults, the more recent Omicron variant did not replicate more efficiently in the NECs than the earlier Delta variant. These data support suggestions that Omicron does not necessarily have a replicative advantage over Delta in the URT of adults [33], and the observed increase in transmission with Omicron in adults is more likely reflective of increased antibody evasion [34–37].

Surprisingly, age-dependent differences in viral replication in NECs were much less pronounced in the case of Omicron. Indeed, there was no notable difference in Omicron RNA titers at 24 h.p.i in adult versus pediatric NECs. These data may provide preliminary evidence that the Omicron variant, at least to some extent, is able to evade aspects of the pediatric innate immune response, as has previously been demonstrated [38]. Whether this is sufficient to result in an increased number of pediatric infections during the Omicron wave [39,40], or whether other factors are more important, remains to be determined. However, it is striking to note (at least in terms of RNA levels) increased titers of Omicron in pediatric NECs compared to infection with Delta and the ancestral virus. These data are consistent with the increased number of pediatric infections observed during the Omicron wave [39,40].

Finally, it is important to recognize the limitations of this study. Due to the difficulties associated with obtaining NECs from children, only a limited number of donors could be used for this study. However, as donors were not selected according to susceptibility to respiratory viral infection, their responses should be broadly representative of healthy children. Furthermore, our data focused on the role of nasal epithelial cells in age-dependent differences in SARS-CoV-2 infection. Nevertheless, there may be other mechanisms to explain the reduced susceptibility of children to SARS-CoV-2 infection that were not measured in the present study. For example, children and adolescents have higher titers of preexisting antibodies to SARS-CoV-2 compared to adults [41]. This study is unable to ascertain if this plays a more significant role than the nasal epithelium in protecting children from infection in vivo.

Materials and methods

Cell collection and ethics statement

Primary NECs were collected from healthy adult (aged 19 to 66 years old) donors by placing a sterile nasal mucosal curette (Arlington Scientific, USA) in the mid-inferior portion of the inferior turbinate during July 2018 to May 2021 (during which time there was only sporadic community cases of COVID-19 in Queensland and Western Australia). Informed consent was obtained from all donors. Primary NECs were obtained from healthy pediatric donors (aged 2 to 11 years old) in the same manner while under general anesthetic prior to ear, nose, and throat (ENT)-related surgeries including tonsillectomies, adenoidectomies, or for sleep apnoea. Children did not have any other unknown underlying condition at the time of recruitment and sampling. This study was approved by the University of Queensland's Human Research Ethics Committee (2020001742), the Queensland Children's Hospital and Health Service Human Research Ethics Committee (HREC/16/QRCH/215, HREC/10/QRCH/78), Queensland University of Technology Human Research Ethics Committee 17000000039), and St John of God Subiaco Hospital Human Ethics Committee as part of the **Western** Australia Epithelial Research Program (WAERP) (Ethics #901). Primary NECs were established as previously described [42–44] and stored in freezing media (FBS with 10% DMSO) at passage 1 or 2. In total, we included 38 donors in this study ($N = 15$ adult (7 females, 8 male, 37.9 ± 16.5 years old) and $N = 23$ pediatric (11 female, 12 male, 5.6 ± 2.7 years old)).

Cell culture

African green monkey kidney epithelial Vero cells were maintained in MEM (Invitrogen), containing 10% (v/v) heat-inactivated fetal bovine serum (Cytiva), 100 U/mL penicillin, and streptomycin (Life Technologies Australia). Cell lines were obtained from American Type Culture Collection (ATCC; Virginia, USA). Primary NECs were expanded and passaged in Pneumacult EX Plus media (STEMCELL Technologies, Canada). After initial expansion, NECs were seeded at a density of 4 to 5×10^5 cells/transwell on 6.5-mm transwell polyester membranes with 0.4 μm pores (Corning Costar, USA) and cultured in EX Plus media (STEMCELL Technologies). Cells were monitored for confluence. When a confluent monolayer was achieved, cells were "air-lifted" by removing the media from the apical chamber and replacing the basolateral media with Pneumacult air liquid interface (ALI) media (STEMCELL Technologies) [45]. Medium was replaced in the basal compartment 3 times a week, and the cells were maintained in ALI conditions for at least 3 weeks until ciliated cells and mucus were observed and cells obtained a transepithelial electrical resistance (TEER) measurement greater than 800 Ω/cm^2. Fully differentiated cultures were used in downstream infection experiments.

Viral stocks

SARS-CoV-2 isolate hCoV-19/Australia/QLD02/2020 (QLD02) (used as the original ancestral virus), hCoV-19/Australia/QLD1893C/2021 (QLD1893C) (GISAID Accession ID; EPI_ISL_2433928; Delta), and hCoV-19/Australia/NSW-RPAH-1933/2021 (GISAID Accession ID; EPI_ISL_6814922; Omicron) were kindly provided by Queensland Health Forensic and Scientific Services, Queensland Department of Health, and the Kirby Institute (in collaboration with NSW Health Pathology). In this setting, we collectively acknowledge the contribution of the scientists and pathologists of NSW Health Pathology and the Kirby Institute to this project. Growth and use of primary isolates was under approval of the NSW Chef Health Officer following independent scientific review. Virus was amplified in Vero cells expressing human TMPRSS2 and titrated by plaque assay [46]. All studies with SARS-CoV-2 were performed under physical containment 3 (PC3) conditions and were approved by the University of Queensland Biosafety Committee (IBC/374B/SCMB/2020).

Viral infection

Differentiated adult and pediatric NECs were infected with mock (PBS), QLD02 (1.25×10^5 PFU or 1.7×10^4 PFU), QLD1517 (1.7×10^4 PFU), or NSW1933 (1.7×10^4 PFU). Specifically, 100 μL of virus or PBS was placed on the epithelial surface in the apical compartment and incubated for 1 hour at 37 ˚C. Following incubation, excess virus was removed from the transwell, and cells were incubated at 37 ˚C with 5% CO_2. Every 24 hours, the basolateral media was refreshed with 1 mL of new ALI media. At predetermined time points, post-infection 100 μL of PBS was added to the apical compartment, and cells were incubated at 37 ˚C with 5% CO_2 for 10 minutes. The apical supernatant was subsequently collected and stored at −80 ˚C. Cells were lysed with Buffer RLT (Qiagen, USA) containing 0.01% β-mercaptoethanol for RNA analysis. Alternatively, cells were lysed in 2% SDS/PBS lysis buffer (2% SDS/PBS buffer, 10% 10× PhosSTOP, 4% 25× protease inhibitor) for protein analysis or fixed overnight in 4% paraformaldehyde for histology.

Histology

Fixed cells on a transwell membrane were routine processed and embedded in paraffin, sectioned at 5 μm, and subsequently stained with hematoxylin–eosin (HE) or periodic acid–Schiff

(PAS). Sections were assessed for cellular morphology by a veterinary pathologist (H.B.O.) blinded to the experimental design.

Immunofluorescence

Differentiated epithelial cells grown on a transwell membrane were fixed with 4% paraformaldehyde (Cat#15710, Electron Microscopy Sciences) in PBS for 45 minutes at room temperature, followed by a blocking with 0.5% BSA (Sigma) in PBS for 30 minutes and permeabilization with 0.02% of Triton X-100 (Sigma) in PBS for 15 minutes at room temperature. After washing twice with PBS/BSA and a second blocking step for 10 minutes at room temperature, samples were incubated with primary antibodies overnight at 4 ˚C. Primary antibodies were diluted in 0.5% BSA in PBS blocking solution: 1:400 ZO-1 (Cat#40–2200, Thermo Fisher Scientific), 1:1,000 MUC5AC (Cat#MA5-12178, Thermo Fisher Scientific), and 1:500 ACE2 (Cat#AF933, R&D Systems). After 3 washing steps with 0.5% BSA/PBS for 5 minutes each time, the samples were incubated in secondary antibody: 1:1,000 Alexa Flour 555 donkey anti-goat (Cat#A21432, Invitrogen) for 2.5 hours at room temperature in dark, and after 3 washes in PBS and 3 washes with 0.5% BSA/PBS, the cells were incubated with a 1:1,000 Alexa Fluor 488 goat anti-mouse (Cat#A32728, Invitrogen) for 2.5 hours at room temperature covered from light. The cells were simultaneously stained with 1:400 Alexa Fluor 647 Phalloidin (Cat#A22287 Invitrogen) and 1:1,000 DAPI. After 3 washes in PBS, the transwell membranes with cells were cut with a scalpel, briefly dipped in milli-q water, and mounted on a class slide using ProLong Gold Antifade Mountant (Cat# P10144, Thermo Fisher Scientific). Mounted samples were imaged on a spinning disk confocal system (Marianas; 3I) consisting of an Axio Observer Z1 (Carl Zeiss) equipped with a CSU-W1 spinning disk head (Yokogawa Corporation of America), ORCA-Flash4.0 v2 sCMOS camera (Hamamatsu Photonics), and 63× 1.4 NA/Plan-Apochromat/180 μm WD objective. Image acquisition was performed using SlideBook 6.0 (3I). A total of 150 optical sections from 5 random regions of interest (ROIs) from each sample were acquired from the top of the differentiated epithelial cells. Image processing was performed using Fiji/ImageJ (Version 2.1.0/1.53c) as follows: Background was reduced using the Substract Backgound 50 pixel rolling ball radius, and the mean fluorescence intensity (MFI, a.u. arbitrary units) was measured from the average intensity images.

Western blotting

For total cell lysates, cells were washed twice with cold PBS and lysed with SDS/PBS lysis buffer (2% SDS/PBS buffer, 10% 10× PhosSTOP, 4% 25× protease inhibitor). Pierce BCA protein assay kit (Thermo Fisher Scientific) was used to equalize protein amounts. After adding LDS buffer (4×) with reducing agent (10×), mix protein samples were subsequently boiled at 100 ˚C for 10 minutes to denature proteins. Proteins were separated on 4% to 15% mini protean TGX precast gels (Biorad) in running buffer (200 mM Glycine, 25 mM Tris, 0.1% SDS (pH 8.6)), transferred to nitrocellulose membrane (Cat#1620112, BioRad) in blot buffer (48 nM Tris, 39 nM Glycine, 0.04% SDS, 20% MeOH), and subsequently blocked with 5% (w/v) BSA in Tris-buffered saline with Tween 20 (TBST) for 30 minutes. The immunoblots were analyzed using primary antibodies incubated overnight at 4 ˚C and secondary antibodies linked to horseradish peroxidase (HRP) (Invitrogen), and after each step, immunoblots were washed 3× with TBST. HRP signals were visualized by enhanced chemiluminescence (ECL) (BioRad) and imaged with an AI600 Chemiluminescent Imager (Cytiva). Primary antibodies include rabbit GAPDH (14C10) monoclonal antibody (1:2,500 dilution, Cat#2118, Cell Signaling Technology), rabbit anti-SARS-CoV-2 nucleoprotein/NP antibody (1:1,000 dilution, Cat#40143-R040, Sino Biological), goat polyclonal ACE2 (1:500 dilution, Cat#AF933, R&D Systems), and rabbit

anti-TMPRSS2 antibody (1:1,000 dilution, Cat#ab109131, Abcam). ImageJ (version 1.53) was used to quantify the protein expression level relative to GAPDH levels.

Cytokine levels

Cytokine levels were measured by AlphaLISA (Perkin Elmer) according to the manufacturer's instructions.

Quantification of infectious virus

SARS-CoV-2 titers in cell culture supernatants were determined by plaque assay on Vero cells, as described previously [46].

RNA extraction and quantitative reverse transcription PCR (qRT-PCR)

RNA was extracted from NECs using Nucleozole reagent according to the manufacturer's instructions, DNA was removed by DNase I (Thermo Fisher Scientific) treatment, and 1-μg DNA-free RNA was reverse transcribed into cDNA using the High Capacity cDNA Reverse Transcription Kit (Applied Biosystems) on a Mastercycler Thermocycler (Eppendorf, Hamburg, Germany) according to the manufacturer's instructions using random primers. Real-time PCR was performed on generated cDNA with SYBER Green (Invitrogen) using QuantStudio 6 Flex Real-Time PCR System, an Applied Biosystems Real-Time PCR Instruments (Thermo Fisher Scientific). Gene expression was normalized relative to glyceraldehyde 3-phosphate dehydrogenase (*GAPDH*) or hypoxanthine-guanine phosphoribosyltransferase (HPRT) expression; fold change was calculated using the ΔΔCt method. All primers used in this study are listed in Table 1.

RNA sequencing

RNA-Seq libraries were prepared using the Illumina stranded total RNA prep ligation with the Ribo-Zero plus kit (Illumina) and IDT for Illumina RNA UD Indexes according to the standard manufacturer's protocol. Briefly, 50 ng of total RNA was depleted of rRNA and then fragmented by heat. cDNA was synthesized from the fragmented RNA using random primers. The first strand cDNA was converted into dsDNA in the presence of dUTP to maintain the "strandedness" of the library. The 3′ ends of the cDNA were adenylated, and pre-index anchors were ligated. The libraries were then amplified with 14 to 16 cycles of PCR incorporating unique indexes for each sample to produce libraries ready for sequencing. The libraries

Table 1. Primers used in the present study.

Primer name	Sequence (5′-3′)
h*IFIT1*	FW:TTGCCTGGATGTATTACCAC RV: GCTTCTTGCAAATGTTCTCC
h*CXCL10*	FW: GTGGCATTCAAGGAGTACCTC RV: GCCTTCGATTCTGGATTCAGACA
h*ISG15*	FW: GAGAGGCAGCGAACTCATCT; RV: CTTCAGCTCTGACACCGACA)
h*GAPDH*	FW: CGAGATCCCTCCAAAATCAA; RV: TTCACACCCATGACGAACAT
h*HPRT*	FW: TCAGGCAGTATAATCCAAAGATGGT RV: AGTCTGGCTTATATCCAACACTTCG
ORF3a	FW: ACAAGCCTCACTCCCTTTCG RV: TGAACACCCTTGGAGAGTGC

https://doi.org/10.1371/journal.pbio.3001728.t001

were quantified on the Perkin Elmer LabChip GX Touch with the DNA High Sensitivity Reagent kit (Perkin Elmer). Libraries were pooled in equimolar ratios, and the pool was quantified by qPCR using the KAPA Library Quantification Kit—Illumina/Universal (KAPA Biosystems) in combination with the Life Technologies Viia 7 real-time PCR instrument.

Sequencing was performed using the Illumina NextSeq500 (NextSeq control software v2.2.0/Real Time Analysis v2.4.11). The library pool was diluted and denatured according to the standard NextSeq protocol and sequenced to generate single-end 76 bp reads using a 75 cycle NextSeq500/550 High Output reagent Kit v2.5 (Illumina). After sequencing, fastq files were generated using bcl2fastq2 (v2.20.0.422), which included trimming the first cycle of the insert read. Library preparation and sequencing was performed at the Institute for Molecular Bioscience Sequencing Facility (University of Queensland).

RNA sequencing analysis

The quality of the trimmed RNA-seq reads was assessed with FastQC [47] and MultiQC [48]. Salmon [49] was used for transcript quantification from human transcriptome (GENCODE Release 36, accessed in December 2020). A decoy aware transcriptome file was created for Salmon transcript quantification followed by the transcriptome index [49]. The R package, DESeq2 [50], was then used for differential gene expression (DGE) analysis and further validated through using the limma R package [51] with Voom transformation [52]. DGEs between virus and mock infected samples were analyzed by controlling the effect of the age group and gender of the individual samples, genes with adjusted *p*-value less than 0.05 were considered significant. Gene set enrichment analysis was performed using the R package GOseq [53]. All the R scripts were run on R-Studio platform (RStudio Team 2020, v 1.4.1717).

Statistical analysis

Where sufficient cell numbers were present, samples were performed in duplicate, and the results were averaged and shown as a single data point. If sufficient cells were not present, a single transwell was used to determine the response of that donor to viral infection. Outliers of continual variables were removed using ROUT's test (Q = 1%). Data were tested for normality using the Shapiro–Wilk test. Where data were normally distributed, data were analyzed using an unpaired 2-tailed Student *t* test. Where data were not normally distributed, data were analyzed using a Mann–Whitney U test. Significance was set at $p < 0.05$. Each donor is shown with a distinct symbol that is used consistently throughout the paper.

Conclusions

The data presented here strongly suggest that the nasal epithelium of children is distinct and that it may afford children some level of protection from ancestral SARS-CoV-2, although such age-dependent differences become less pronounced in the case of Omicron infection.

Supporting information

S1 Fig. Pediatric nasal epithelial cells display pseudocysts. Representative HE-stained section of pediatric NECs culture differentiated at an air–liquid interface. Scale bar is equivalent of 150 μm. HE, hematoxylin–eosin; NEC, nasal epithelial cell.
(TIF)

S2 Fig. Relative SARS-CoV-2 NP levels compared to GAPDH in pediatric and adult NECs. Western blot of adults and pediatric donors blotted for SARS-CoV-2 N at various time points post-infection; $N = 5$ adults (3 females, 2 males) and $N = 8$ children (4 females, 4 males). * NP

levels of Pediatric donor 4 at 24 h.p.i are missing. Data are contained in S1 Data and raw western blot images are available in S1 Raw image. GAPDH, glyceraldehyde 3-phosphate dehydrogenase; h.p.i, hours post-infection; NEC, nasal epithelial cell; NP, nucleoprotein; SARS-CoV-2, Severe Acute Respiratory Syndrome Coronavirus 2.
(TIF)

S3 Fig. Relative ACE2 levels compared to GAPDH in pediatric and adult NECs. Western blot of adults and pediatric donors blotted for ACE at 24 h.p.i; $N = 3$ adults (1 females, 2 males) and $N = 5$ children (3 females, 2 males). Data are contained in S1 Data and raw western blot images are available in S1 Raw images. ACE2, angiotensin-converting enzyme 2; GAPDH, glyceraldehyde 3-phosphate dehydrogenase; h.p.i, hours post-infection; NEC, nasal epithelial cell; SARS-CoV-2, Severe Acute Respiratory Syndrome Coronavirus 2.
(TIF)

S1 Table. DEGs of infected pediatric NECs (72 h.p.i) compared to adult cells with statistics. DEGs were identified using DESeq2, genes with adjusted *p*-value less than 0.05 value were considered significant. DEG, differentially expressed gene; h.p.i, hours post-infection; NEC, nasal epithelial cell.
(DOCX)

S2 Table. DEGs of infected pediatric NECs (72 h.p.i) compared to adult cells with statistics. DEGs were identified using limma, genes with adjusted *p*-value less than 0.05 value were considered significant. DEG, differentially expressed gene; h.p.i, hours post-infection; NEC, nasal epithelial cell.
(DOCX)

S1 Data. Raw data for figures used in the manuscript.
(PDF)

S1 Raw images. The original, uncropped images supporting the western blot in Figs 1E, 2B, S2 and S3.
(RAR)

Acknowledgments

We greatly thank the participants in the study and the members of the research team. The authors thank the participants and their families in the Western Australian Epithelial Research Program (WAERP) for their contribution to this study. Current members of WAERP include: Anthony Kicic, Stephen M. Stick, Elizabeth Kicic-Starcevich, Amy Greenly, Angela Fuery, Luke W. Garratt, Erika N. Sutanto, Kevin Looi, Jessica Hillas, Thomas Iosifidis, Craig Schofield, Samantha McLean, Luke Berry, Samuel T. Montgomery, Kak-Ming Ling, Renee Ng, Andrew Vaitekenas, Daniel Laucirica, Matthew Poh, Reanne Ho, Joshua Iszatt, Katherine Landwehr, Denby Evans, Rebecca Watkinson, Patricia Agudelo-Romero, Jose Caparros-Martin, Alexander de Bont, Julia Maynard, Rohan Flint, Jack Canning, Shyan Vijayasekaran, George Sim, Mairead Heaney, Tom Rawlings, Neil Chambers, Christopher Johnson, Eugene Roscioli, Alexander Larcombe, Tim Barnett, Rael, Rivers, and Kate McGee.

Author Contributions

Conceptualization: Asha C. Bowen, Kirsten M. Spann, Kirsty R. Short.

Data curation: Yanshan Zhu, Keng Yih Chew, Anjana C. Karawita.

Funding acquisition: Kirsty R. Short.

Investigation: Yanshan Zhu, Keng Yih Chew, Melanie Wu, Anjana C. Karawita, Georgina McCallum, Xiaohui Wang, Julian D. J. Sng.

Methodology: Yanshan Zhu, Keng Yih Chew, Ayaho Yamamoto, Larisa I. Labzin, Tejasri Yarlagadda, Claudia J. Stocks, Yao Xia, Tobias R. Kollmann, David Martino, Merja Joensuu, Frédéric A. Meunier, Giuseppe Balistreri, Helle Bielefeldt-Ohmann, Anthony Kicic, Peter D. Sly, Kirsten M. Spann, Kirsty R. Short.

Project administration: Anthony Kicic, Kirsty R. Short.

Resources: Anthony Kicic.

Supervision: Alexander A. Khromykh, Asha C. Bowen, Kirsten M. Spann, Kirsty R. Short.

Validation: Yanshan Zhu, Keng Yih Chew, Melanie Wu, Georgina McCallum, Lauren E. Steele, Merja Joensuu, Giuseppe Balistreri.

Visualization: Yanshan Zhu, Keng Yih Chew, Anjana C. Karawita, Merja Joensuu, Giuseppe Balistreri, Helle Bielefeldt-Ohmann.

Writing – original draft: Yanshan Zhu, Kirsty R. Short.

Writing – review & editing: Yanshan Zhu, Kirsty R. Short.

References

1. Lu X, Zhang L, Du H, Zhang J, Li YY, Qu J, et al. SARS-CoV-2 Infection in Children. N Engl J Med. 2020; 382(17):1663–1665. https://doi.org/10.1056/NEJMc2005073 PMID: 32187458.
2. Zhu Y, Bloxham CJ, Hulme KD, Sinclair JE, Tong ZWM, Steele LE, et al. A Meta-analysis on the Role of Children in Severe Acute Respiratory Syndrome Coronavirus 2 in Household Transmission Clusters. Clin Infect Dis. 2021; 72(12):e1146–e1153. https://doi.org/10.1093/cid/ciaa1825 PMID: 33283240.
3. Goldstein E, Lipsitch M, Cevik M. On the Effect of Age on the Transmission of SARS-CoV-2 in Households, Schools, and the Community. J Infect Dis. 2021; 223(3):362–369. https://doi.org/10.1093/infdis/jiaa691 PMID: 33119738.
4. Hua C-Z, Miao Z-P, Zheng J-S, Huang Q, Sun Q-F, Lu H-P, et al. Epidemiological features and viral shedding in children with SARS-CoV-2 infection. J Med Virol. 2020; 92(11):2804–12. https://doi.org/10.1002/jmv.26180 PMID: 32542750.
5. Kim YI, Yu KM, Koh JY, Kim EH, Kim SM, Kim EJ, et al. Age-dependent pathogenic characteristics of SARS-CoV-2 infection in ferrets. Nat Commun. 2022; 13(1):21. https://doi.org/10.1038/s41467-021-27717-3 PMID: 35013229.
6. Bunyavanich S, Do A, Vicencio A. Nasal Gene Expression of Angiotensin-Converting Enzyme 2 in Children and Adults. JAMA. 2020; 323(23):2427–2429. https://doi.org/10.1001/jama.2020.8707 PMID: 32432657.
7. Pierce CA, Sy S, Galen B, Goldstein DY, Orner E, Keller MJ, et al. Natural mucosal barriers and COVID-19 in children. JCI Insight. 2021; 6(9). https://doi.org/10.1172/jci.insight.148694 PMID: 33822777.
8. Wark PAB, Pathinayake PS, Kaiko G, Nichol K, Ali A, Chen L, et al. ACE2 expression is elevated in airway epithelial cells from older and male healthy individuals but reduced in asthma. Respirology. 2021; 26(5):442–451. https://doi.org/10.1111/resp.14003 PMID: 33455043.
9. Hoffmann M, Kleine-Weber H, Schroeder S, Krüger N, Herrler T, Erichsen S, et al. SARS-CoV-2 Cell Entry Depends on ACE2 and TMPRSS2 and Is Blocked by a Clinically Proven Protease Inhibitor. Cell. 2020; 181(2):271–80.e8. https://doi.org/10.1016/j.cell.2020.02.052 PMID: 32142651.
10. Saheb Sharif-Askari N, Saheb Sharif-Askari F, Alabed M, Temsah M-H, Al Heialy S, Hamid Q, et al. Airways Expression of SARS-CoV-2 Receptor, ACE2, and TMPRSS2 Is Lower in Children Than Adults and Increases with Smoking and COPD. Mol Ther Methods Clin Dev. 2020; 18:1–6. https://doi.org/10.1016/j.omtm.2020.05.013 PMID: 32537478.

11. Maughan EF, Nigro E, Pennycuick A, Gowers KHC, Denais C, Gómez-López S, et al. Cell-intrinsic differences between human airway epithelial cells from children and adults. bioRxiv. 2020:2020.04.20.027144. https://doi.org/10.1101/2020.04.20.027144

12. Loske J, Röhmel J, Lukassen S, Stricker S, Magalhães VG, Liebig J, et al. Pre-activated antiviral innate immunity in the upper airways controls early SARS-CoV-2 infection in children. Nat Biotechnol. 2022; 40(3):319–324. https://doi.org/10.1038/s41587-021-01037-9 PMID: 34408314.

13. Lucas C, Wong P, Klein J, Castro TBR, Silva J, Sundaram M, et al. Longitudinal analyses reveal immunological misfiring in severe COVID-19. Nature. 2020; 584(7821):463–469. https://doi.org/10.1038/s41586-020-2588-y PMID: 32717743.

14. Short KR, Kroeze EJBV, Fouchier RAM, Kuiken T. Pathogenesis of influenza-induced acute respiratory distress syndrome. Lancet Infect Dis. 2014; 14(1):57–69. https://doi.org/10.1016/S1473-3099(13)70286-X PMID: 24239327.

15. Diamond MS, Kanneganti TD. Innate immunity: the first line of defense against SARS-CoV-2. Nat Immunol. 2022; 23(2):165–176. https://doi.org/10.1038/s41590-021-01091-0 PMID: 35105981.

16. Felgenhauer U, Schoen A, Gad HH, Hartmann R, Schaubmar AR, Failing K, et al. Inhibition of SARS-CoV-2 by type I and type III interferons. J Biol Chem. 2020; 295(41):13958–13964. https://doi.org/10.1074/jbc.AC120.013788 PMID: 32587093.

17. Rajah MM, Hubert M, Bishop E, Saunders N, Robinot R, Grzelak L, et al. SARS-CoV-2 Alpha, Beta, and Delta variants display enhanced Spike-mediated syncytia formation. EMBO J. 2021; 40(24): e108944. https://doi.org/10.15252/embj.2021108944 PMID: 34601723.

18. Khateeb J, Li Y, Zhang H. Emerging SARS-CoV-2 variants of concern and potential intervention approaches. Crit Care. 2021;12; 25(1):244. https://doi.org/10.1186/s13054-021-03662-x PMID: 34253247.

19. Chen F, Tian Y, Zhang L, Shi Y. The role of children in household transmission of COVID-19: a systematic review and meta-analysis. Int J Infect Dis. 2022; 122:266–275. https://doi.org/10.1016/j.ijid.2022.05.016 PMID: 35562045.

20. Ogata T, Tanaka H, Nozawa Y, et al. Increased Secondary Attack Rate among Unvaccinated Household Contacts of Coronavirus Disease 2019 Patients with Delta Variant in Japan. Int J Environ Res Public Health. 2022; 19(7):3889. https://doi.org/10.3390/ijerph19073889 PMID: 35409572.

21. Cloete J, Kruger A, Masha M, du Plessis NM, Mawela D, Tshukudu M, et al. Paediatric hospitalisations due to COVID-19 during the first SARS-CoV-2 omicron (B.1.1.529) variant wave in South Africa: a multicentre observational study. Lancet Child Adolesc Health. 2022. https://doi.org/10.1016/S2352-4642(22)00027-X PMID: 35189083.

22. Marks KJ, Whitaker M, Anglin O, Milucky J, Patel K, Pham H, et al. Hospitalizations of Children and Adolescents with Laboratory-Confirmed COVID-19—COVID-NET, 14 States, July 2021-January 2022. MMWR Morb Mortal Wkly Rep. 2022; 71(7):271–278. https://doi.org/10.15585/mmwr.mm7107e4 PMID: 35176003.

23. Yi H, Wang J, Wang J, Lu Y, Zhang Y, Peng R, et al. The Emergence and Spread of Novel SARS-CoV-2 Variants. Front Public Health. 2021; 9:696664. https://doi.org/10.3389/fpubh.2021.696664 PMID: 34409009.

24. Bardanzellu F, Fanos V. How could metabolomics change pediatric health? Ital J Pediatr. 2020; 46(1):37. https://doi.org/10.1186/s13052-020-0807-7 PMID: 32216818.

25. Yazicioglu T, Mühlfeld C, Autilio C, Huang CK, Bär C, Dittrich-Breiholz O, et al. Aging impairs alveolar epithelial type II cell function in acute lung injury. Am J Physiol Lung Cell Mol Physiol. 2020; 319(5): L755–l69. https://doi.org/10.1152/ajplung.00093.2020 PMID: 32877222.

26. Lachassinne E, de Pontual L, Caseris M, Lorrot M, Guilluy C, Naud A, et al. SARS-CoV-2 transmission among children and staff in daycare centres during a nationwide lockdown in France: a cross-sectional, multicentre, seroprevalence study. Lancet Child Adolesc Health. 2021; 5(4):256–264. https://doi.org/10.1016/S2352-4642(21)00024-9 PMID: 33571450.

27. Stringhini S, Wisniak A, Piumatti G, Azman AS, Lauer SA, Baysson H, et al. Seroprevalence of anti-SARS-CoV-2 IgG antibodies in Geneva, Switzerland (SEROCoV-POP): a population-based study. Lancet. 2020; 396(10247):313–319. https://doi.org/10.1016/S0140-6736(20)31304-0 PMID: 32534626.

28. Tönshoff B, Müller B, Elling R, Renk H, Meissner P, Hengel H, et al. Prevalence of SARS-CoV-2 Infection in Children and Their Parents in Southwest Germany. JAMA Pediatr. 2021; 175(6):586–593. https://doi.org/10.1001/jamapediatrics.2021.0001 PMID: 33480966.

29. Hasan MR, Ahmad MN, Dargham SR, Zayed H, Al Hashemi A, Ngwabi N, et al. Nasopharyngeal Expression of Angiotensin-Converting Enzyme 2 and Transmembrane Serine Protease 2 in Children within SARS-CoV-2-Infected Family Clusters. Microbiol Spectr. 2021; 9(3):e0078321. https://doi.org/10.1128/Spectrum.00783-21 PMID: 34730438.

30. Mehta NS, Mytton OT, Mullins EWS, Fowler TA, Falconer CL, Murphy OB, et al. SARS-CoV-2 (COVID-19): What Do We Know About Children? A Systematic Review. Clin Infect Dis. 2020; 71(9):2469–2479. https://doi.org/10.1093/cid/ciaa556 PMID: 32392337.

31. Zimmermann P, Curtis N. Why is COVID-19 less severe in children? A review of the proposed mechanisms underlying the age-related difference in severity of SARS-CoV-2 infections. Arch Dis Child. 2020 Dec 1:archdischild-2020-320338. https://doi.org/10.1136/archdischild-2020-320338 PMID: 33262177.

32. Mlcochova P, Kemp SA, Dhar MS, Papa G, Meng B, Ferreira IA, et al. SARS-CoV-2 B. 1.617. 2 Delta variant replication and immune evasion. Nature. 2021; 599(7883):114–119. https://doi.org/10.1038/s41586-021-03944-y PMID: 34488225.

33. Zhao H, Lu L, Peng Z, Chen LL, Meng X, Zhang C, et al. SARS-CoV-2 Omicron variant shows less efficient replication and fusion activity when compared with Delta variant in TMPRSS2-expressed cells. Emerg Microbes Infect. 2022; 11(1):277–283. https://doi.org/10.1080/22221751.2021.2023329 PMID: 34951565.

34. Meng B, Abdullahi A, Ferreira I, Goonawardane N, Saito A, Kimura I, et al. Altered TMPRSS2 usage by SARS-CoV-2 Omicron impacts infectivity and fusogenicity. Nature. 2022; 603(7902):706–714. https://doi.org/10.1038/s41586-022-04474-x PMID: 35104837.

35. Hoffmann M, Krüger N, Schulz S, Cossmann A, Rocha C, Kempf A, et al. The Omicron variant is highly resistant against antibody-mediated neutralization: Implications for control of the COVID-19 pandemic. Cell. 2022; 185(3):447–56.e11. https://doi.org/10.1016/j.cell.2021.12.032 PMID: 35026151.

36. Puhach O, Adea K, Hulo N, Sattonnet P, Genecand C, Iten A, et al. Infectious viral load in unvaccinated and vaccinated individuals infected with ancestral, Delta or Omicron SARS-CoV-2. Nat Med. 2022. https://doi.org/10.1038/s41591-022-01816-0 PMID: 35395151.

37. Petros BA, Turcinovic J, Welch NL, White LF, Kolaczyk ED, Bauer MR, et al. Early introduction and rise of the Omicron SARS-CoV-2 variant in highly vaccinated university populations. Clin Infect Dis. 2022 May 25:ciac413. Epub ahead of print. https://doi.org/10.1093/cid/ciac413 PMID: 35616119.

38. Shalamova L, Felgenhauer U, Wilhelm J, Schaubmar AR, Büttner K, Schoen A, et al. Omicron variant of SARS-CoV-2 exhibits an increased resilience to the antiviral type I interferon response. PNAS Nexus. 2022. https://doi.org/10.1093/pnasnexus/pgac067

39. Baker JM, Nakayama JY, O'Hegarty M, McGowan A, Teran RA, Bart SM, et al. SARS-CoV-2 B.1.1.529 (Omicron) Variant Transmission Within Households—Four U.S. Jurisdictions, November 2021-February 2022. MMWR Morb Mortal Wkly Rep. 2022; 71(9):341–6. https://doi.org/10.15585/mmwr.mm7109e1 PMID: 35238860.

40. Belay ED, Godfred-Cato S. SARS-CoV-2 spread and hospitalisations in paediatric patients during the omicron surge. Lancet Child Adolesc Health. 2022. https://doi.org/10.1016/S2352-4642(22)00060-8 PMID: 35189084.

41. Ng KW, Faulkner N, Cornish GH, Rosa A, Harvey R, Hussain S, et al. Preexisting and de novo humoral immunity to SARS-CoV-2 in humans. Science. 2020; 370(6522):1339–1343. https://doi.org/10.1126/science.abe1107 PMID: 33159009.

42. Kicic A, Hallstrand TS, Sutanto EN, Stevens PT, Kobor MS, Taplin C, et al. Decreased fibronectin production significantly contributes to dysregulated repair of asthmatic epithelium. Am J Respir Crit Care Med. 2010; 181(9):889–898. https://doi.org/10.1164/rccm.200907-1071OC PMID: 20110557.

43. Kicic A, Stevens PT, Sutanto EN, Kicic-Starcevich E, Ling KM, Looi K, et al. Impaired airway epithelial cell responses from children with asthma to rhinoviral infection. Clin Exp Allergy. 2016; 46(11):1441–1455. https://doi.org/10.1111/cea.12767 PMID: 27238549.

44. Spann KM, Baturcam E, Schagen J, Jones C, Straub CP, Preston FM, et al. Viral and host factors determine innate immune responses in airway epithelial cells from children with wheeze and atopy. Thorax. 2014; 69(10):918–925. https://doi.org/10.1136/thoraxjnl-2013-204908 PMID: 24811725.

45. Hou YJ, Okuda K, Edwards CE, Martinez DR, Asakura T, Dinnon KH 3rd, et al. SARS-CoV-2 Reverse Genetics Reveals a Variable Infection Gradient in the Respiratory Tract. Cell. 2020; 182(2):429–46.e14. https://doi.org/10.1016/j.cell.2020.05.042 PMID: 32526206.

46. Gordon DE, Jang GM, Bouhaddou M, Xu J, Obernier K, White KM, et al. A SARS-CoV-2 protein interaction map reveals targets for drug repurposing. Nature. 2020; 583(7816):459–468. https://doi.org/10.1038/s41586-020-2286-9 PMID: 32353859.

47. S A. FastQC: a quality control tool for high throughput sequence data. http://www.bioinformatics.babraham.ac.uk/projects/fastqc. Jan 2020.

48. Ewels P, Magnusson M, Lundin S, Käller M. MultiQC: summarize analysis results for multiple tools and samples in a single report. Bioinformatics. 2016; 32(19):3047–3048. https://doi.org/10.1093/bioinformatics/btw354 PMID: 27312411.

49. Patro R, Duggal G, Love MI, Irizarry RA, Kingsford C. Salmon provides fast and bias-aware quantification of transcript expression. Nat Methods. 2017; 14(4):417–419. https://doi.org/10.1038/nmeth.4197 PMID: 28263959.

50. Love MI, Huber W, Anders S. Moderated estimation of fold change and dispersion for RNA-seq data with DESeq2. Genome Biol. 2014; 15(12):550. https://doi.org/10.1186/s13059-014-0550-8 PMID: 25516281.

51. Ritchie ME, Phipson B, Wu D, Hu Y, Law CW, Shi W, et al. limma powers differential expression analyses for RNA-sequencing and microarray studies. Nucleic Acids Res. 2015; 43(7):e47. https://doi.org/10.1093/nar/gkv007 PMID: 25605792.

52. Law CW, Chen Y, Shi W, Smyth GK. voom: Precision weights unlock linear model analysis tools for RNA-seq read counts. Genome Biol. 2014; 15(2):R29. https://doi.org/10.1186/gb-2014-15-2-r29 PMID: 24485249.

53. Young MD, Wakefield MJ, Smyth GK, Oshlack A. Gene ontology analysis for RNA-seq: accounting for selection bias. Genome Biol. 2010; 11(2):R14. https://doi.org/10.1186/gb-2010-11-2-r14 PMID: 20132535.